Joint Centre for Mesoscale Meteorology, Reading, UK

A North Atlantic Survey of Cyclogenesis in 1999: Unified Model Performance in Short Range Forecasts & The Relationship Between Potential Vorticity, Water Vapour Imagery and Analysis Accuracy

A. Semple

Internal Report No. 127
NWP Technical Paper No. 348

March 2001

Met Office Joint Centre for Mesoscale Meteorology Department of Meteorology
University of Reading PO Box 243 Reading RG6 6BB United Kingdom
Tel: +44 (0)118 931 8425 Fax: +44 (0)118 931 8791
www.metoffice.com

Designed and produced by the Met Office © Crown copyright 2001 01/0240 The Met Office logo is a registered trademark.

A North Atlantic Survey of Cyclogenesis in 1999: Unified Model Performance in Short Range Forecasts & The Relationship Between Potential Vorticity, Water Vapour Imagery and Analysis Accuracy.

Adrian Semple

March 2001

Abstract

A relationship has been reported between the upper level Potential Vorticity (PV) model field and radiances observed by Water Vapour (WV) Imagery. This relationship has been used by some authors to identify numerical model errors and then to either infer modifications to the model PV distribution, or to alert operational forecasters that the reliability of the model analysis may be in question. This report documents a cyclogenesis survey that was carried out in order to assess the relationship in terms of its reliability in determining model errors. It shows that although the relationship is verified by the results, the PV&WV comparisons are probabilistic in nature and should not be used as a sole source of information.

The survey data has also been used to observe the Met Office's Unified Model performance in short range forecasts. The results show that the model significantly under-develops most extra-tropical cyclones classified as anything above 'explosive' (corresponding to a deepening rate of 1mb/hour over 24 hours). These explosive cyclones constitute approximately 25% of the cyclone cases studied in this survey.

1 INTRODUCTION 2

2 THE NORTH ATLANTIC CYCLONE SURVEY 4

2.1 RATIONALE 4
2.2 METHOD SPECIFICS 4
2.3 SURVEY RESULTS – INFERENCE OF INITIAL ANALYSIS ACCURACY 6
2.4 SURVEY RESULTS – MODEL PERFORMANCE 9

3 ASSESSMENT OF THE POTENTIAL VORTICITY AND WATER VAPOUR IMAGERY RELATIONSHIP 12

3.1 CHOICE OF POTENTIAL VORTICITY SURFACE USED IN THE WATER VAPOUR COMPARISON 12
3.2 FEATURES OF PV AND WV COMPARISONS 14
3.3 ASSESSMENT OF THE PV & WV RELATIONSHIP 16
3.3.1 Grading the PV & WV Comparisons 16
3.3.2 PV & WV Grading as a Function of the Pressure Error 18
3.3.3 PV & WV Grading as a function of the Location Error. 20
3.3.4 PV & WV Comparisons within the Analysis Classes 22

4 SUMMARY & CONCLUSIONS 24

5 RECOMMENDATIONS 26

6 REFERENCES. 27

1 Introduction

Since its first use by Rossby in 1940, and especially in recent years, Potential vorticity (PV) has become a widely used mathematical concept used in the diagnosis of atmospheric dynamics (Thorpe & Volkert, 1997 provides a short history of its uses). Hoskins et al. (1985) contributed significantly to the modern use of PV through their review of the use and significance of isentropic PV maps. In particular, the importance and relationship of PV to perturbations in the tropopause, and then specifically in extra-tropical cyclones was considered.

Potential Vorticity may be considered as a quantity that combines the vorticity and static stability of the atmosphere. Its importance is a result of two key properties: conservation and invertibility. PV is conserved for adiabatic frictionless flow. This means that as parcels of air descend or ascend along isentropes in the atmosphere, the PV associated with that parcel of air is conserved. This allows the identification and tracking of PV anomalies (i.e. PV features different in value from their surroundings) in time and space. Then, given suitable boundary conditions, the conserved PV of an atmospheric feature may be 'inverted' back to its component wind and temperature fields, and thus all other dynamical fields.

It is this dynamical consistency of PV and the fact that it allows atmospheric features to be tracked in the model, that has led to the comparison of PV fields with water vapour (WV) satellite imagery. WV imagery shows radiances measured in the water vapour absorption band (5.7-7.1 μm) emitted by the Earth-atmosphere system. WV radiances are continuously emitted and reabsorbed vertically, so that only the upper levels of atmospheric water vapour content contribute to the water vapour radiance. In cloud free conditions the radiance corresponds to the atmosphere's net water vapour content in a layer from ~500-700mb (dependent on the moisture content) to ~250mb, so that there is little measure of the water vapour content from the lowest levels of the troposphere. In cloudy conditions, the re-absorption property means that only the upper layer of cloud in the atmosphere actually contributes to the WV image. WV images of the atmosphere are therefore often dominated by high contrasts between dry areas ('low' in the troposphere), and moist areas ('high' in the troposphere).

The location of the atmosphere where this contrast is very apparent is in extra-tropical cyclones. Cyclogenesis involves large scale ascent and descent in characteristic structures within the cyclone (See e.g. Browning et al., 1994 and Semple, 1998). In particular, the 'dry intrusion' is a region which descends from the lower stratosphere/upper troposphere to the rear of the cyclone. Because of its stratospheric origins, the dry intrusion is characterised both by very dry air and by high PV. As it is very dry, the water vapour radiance measured by the satellite originates largely from lower in the troposphere, below the level from which the dry intrusion is descending. In contrast, the cloud band of the cyclone with which it interacts, is very moist and of low PV. The origin of the WV radiances in these areas is therefore in the upper troposphere. The interface between the dry intrusion and other cloudy areas of the cyclone are therefore characterised by both a high contrast in PV values and a high contrast in water vapour radiances.

For these reasons, it is therefore not surprising that a relationship has been observed between upper tropospheric PV fields and WV imagery. This relationship has been exploited so as to detect deviations in the model PV field away from that which is expected and have then been interpreted as the signature of errors in the model representation of that region of the atmosphere. Mansfield (1996, 1997) reports on a project designed to evaluate the use of potential vorticity as an operational forecast tool, and investigates various ways of making the PV/WV comparisons (discussed in Section 3.1). Demirtas and Thorpe (1997) use the relationship to test the sensitivity of short-range weather forecasts to local PV modifications. Based on perceived mismatches between PV and WV imagery, Demirtas and Thorpe

modified the PV fields to provide dynamically consistent model fields from which model re-runs were performed. One case of particular importance significantly improved the subsequent forecast, and has been used as a benchmark case in the study documented in this work.

Based on the positive results of this study, Swarbrick (1999) performed further investigations with a significant number of cases. Swarbrick found however that although some minor positive impacts in the correction of poor forecasts were achieved via modification of PV fields, the results were in general neutral. Swarbrick also commented on how difficult it was to judge whether modifications to the PV field were necessary, and whether any modifications would have an impact on the subsequent forecast.

This report documents work carried out in order to specifically address the following aspects:

- To verify that a relationship exists between upper tropospheric model PV and WV imagery.
- To assess the robustness of the relationship and give an indication as to its reliability.
- To determine if a correlation exists between the quality of the initial analysis, the accuracy of the subsequent forecast and the 'closeness' of the perceived match between PV/WV at the initial analysis time.

The aims of this project therefore required a knowledge and measure of the analysis and forecast accuracy in a significant number of cyclogenesis cases. To facilitate this, a daily cyclogenesis study was carried out within the area of the North Atlantic. This survey produced an interesting view of the performance of the Met Office's model and data assimilation systems throughout a year. The rationale, details and results of this survey are discussed in the following section.

2 The North Atlantic Cyclone Survey

2.1 Rationale

In any forecast the principle contributions to forecast errors will be either due to

(1) imperfections in the model formulation, and/or
(2) errors in the initial analysis

The relative contribution from these two factors to the overall forecast error will vary according to each particular case, depending upon the predictability of the atmospheric state and the sensitivity of the forecast to the initial conditions. However, although errors in the initial analysis (2) will nearly always be a major factor in forecast accuracy, the contribution from the model (1) relative to (2) is also likely to vary depending on the forecast range: short period forecasts errors are more likely to have a smaller contribution from (1) simply by virtue of the shorter period of activity of the model, whilst longer period forecasts will probably have an increased contribution from (1).

The Survey discussed in this work concerns the performance of the model in the short period forecast of T+12. This forecast range was chosen so that over a large number of cases, one would be sure of a significant contribution to the forecast error from the initial analysis (2) relative to the contribution to the forecast error from the model (1). This information could then be used to give some indication of whether that initial analysis was likely to be accurate or inaccurate.

The contribution to the forecast error from the model (1) will still contribute to the overall forecast error. The two contributions (1) and (2) may be partially untangled by the way in which the survey data is analysed. The Survey grades the forecast accuracy on the basis of forecast error in terms of Pressure error and location error relative to the verifying analysis. It is argued that a plot of this data in its pure form (pressure error, location error) will not separate any contribution of (1) and (2) as it is simply a measure of how accurate the forecast was in each case.

However, if one considers rate of change characteristics of the forecast cyclones (i.e. quantities that are dependent on the evolution of the model forecast, as opposed to a measure of its final outcome) then the model trends within the data become more evident.

2.2 Method Specifics

The approach taken was to daily monitor the north Atlantic region for cyclogenesis events. The model performance over a 12 hour period was assessed by comparing the T+12 forecast of a selected cyclone in terms of its position and pressure with that for the cyclone in the verifying analysis (Figure 1).

Cases were then specifically chosen based on the following criteria.

- There was a 'closed low' in the T+0 model analysis mean-sea-level pressure field.
- There was a 'closed low' in the T+12 model forecast mean-sea-level pressure field.
- There was a cloud head visible in the infra-red satellite imagery at the forecast time, T+12 (to allow an estimate of the system size, discussed below).

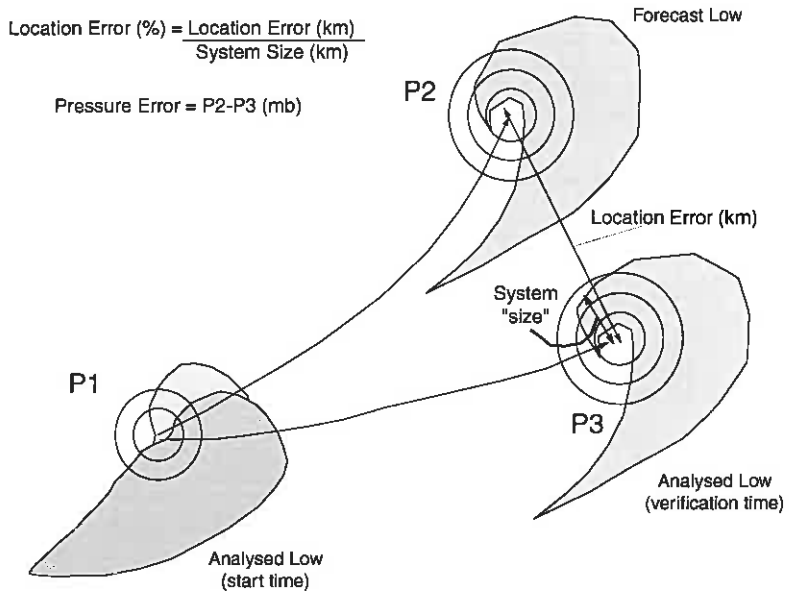

Figure 1 The method used to carry out the cyclogenesis survey. The location error is determined from the direct distance between the centres of the two low pressure fields in the model. An estimate of the system size in this work is determined by a line drawn from the centre of the analysed low to the outer edge of the cloud head on the imagery. The location error may then be expressed relative to the system size (%). The pressure error is determined by the difference between the forecast pressure and verification analysis pressure at the low centres.

In assessment of the T+12 forecast, the pressure and location of the forecast cyclone is measured relative to the analysed pressure and location of the selected cyclone. This introduces a third source of error into the survey method:

(3) errors in the verifying analysis

Cyclones after 12 hours of evolution are generally larger and more developed than those at the initial analysis time. Errors introduced into the method via contribution (3) are therefore likely to be smaller than (1) and (2). This may be an oversimplification in a minority of cases, but it should be stressed that within the confines of the survey, the verifying analysis is the best estimate of the true state of the atmosphere at any one time.

The quality of the short period forecast for the cyclone has been assessed in terms of both its pressure and location error with respect to the verifying analysis. The pressure error is simply the difference in mean sea level pressure at the centre of the low pressure field in the two analyses. In estimating the location error, the actual location error between the two low pressure centres is expressed as a percentage of the size of the developing cyclone at the verification time. The size of the cyclone was estimated in this study as the distance from the centre of the low in the model verification analysis to the outer edge of the cloud head in the satellite imagery (again, this assumes the errors due to the verification analysis (3) are relatively small). This has been used to take account of the fact that smaller systems, with a small absolute location error, actually represent a relatively large location error for that cyclone. Conversely, very large systems with a larger absolute location error represent a relatively small location error.

2.3 *Survey Results – Inference of Initial Analysis Accuracy*

As discussed earlier, the survey results may be used to infer the likely accuracy of the initial analysis from which the forecast was run. The relevant information from the survey data for these purposes is therefore the magnitude of the T+12 forecast pressure and location error relative to the verifying analysis, the result of which is the scatter plot shown in Figure 2. Each cyclone has been given the additional label of the development type according to Young's Scheme of Cyclone Classification (Young et al. 1987, see caption of the figure for details). This information was incorporated into the survey at the onset to allow for any trend to be shown should particular 'modes of evolution' of cyclone development be better forecast than any other. In the event, there was no such trend observed.

As discussed earlier, although the main contribution to the T+12 forecast is expected to be generally from the initial analysis when looking at a large number of cases, this is not expected to be true in 100% of case studies due to some instances in which the model error actually contributes more. To allow for this, the T+12 forecast accuracy has been divided into 'classes' with Class I cyclones representing those in which the initial analysis is likely to be very good, through to Class VI cyclones representing those in which the initial analysis is likely to be very poor. These classes effectively represent bands of forecast accuracy within which one would expect some variation in the error contribution (due to a relative increased contribution by factor (1)), but where the general assumptions concerning error contribution will be true when traversing from one band to another. In essence, we are concerned more with the average characteristics of each class, and we would expect there to be some anomalies within that class.

The figure shows that a significant number of cyclogenesis cases are located towards the bottom left of the graph as Class I cyclones. These contribute 49% to the total number of cyclones in the survey, and indicate a bias towards good short period forecasts and therefore likely good initial analyses. Class II cyclones contribute a further 26% to the cyclone survey. This class of cyclone are considered still relatively good, although clearly there is some indication that initial analysis errors are becoming significant.

Class III cyclones represent 16% of the total survey study. Pressure errors of 8mb or location errors of 45% are considered significant errors in a 12 hour forecast. Initial analysis errors are very likely to be playing an important role in the origins of these poor forecast.

Class IV Cyclones represent 6% of cyclones in the survey. In a 12 hour forecast, pressure errors approaching 12mb have been observed, and represent gross forecast errors. Cyclones with pressure errors of this magnitude in 12 hours are likely to be completely misrepresented in their severity in longer term forecasts.

No Class V cyclones were observed in this study. Class VI cyclones contribute only 3% to the total cyclone survey. However, the errors with which these cyclones are represented (in excess of 21mb in 12 hours) indicate complete forecast 'busts' and represent a huge failure of the Numerical Weather Prediction system. Class IV to VI cyclones, although only representing a total of 8% of the cyclone study, are often considered the most important area in which to improve the model and data assimilation systems, as these cyclones naturally carry with them the greatest risk of damage and loss of life.

Two test cases have been included on the figure for purposes of verification of the survey method (square symbols and labelled Fxddmmyy). Fa160295 refers to a study (Demirtas and Thorpe, 1997) in which a poor forecast of a cyclone was partially corrected by a modification to the PV field based on the PV/WV comparison. As a clear signal in the PV/WV relationship had been reported, and given that this case represented a Class V cyclone, this indicates good performance of the survey method. Fb231299 represents the storm which

crossed the UK on Christmas Eve 1997 (Semple, Saunders and Bader 2001). This storm was found to be represented by very poor forecasts and a poor PV/WV signature in the study. As such, it is fitting that it is represented as a Class VI cyclone.

The results of this survey in terms of its initial analysis accuracy will be used in Sec. 3 as a basis on which to test if there is any relationship between the model potential vorticity and water vapour imagery.

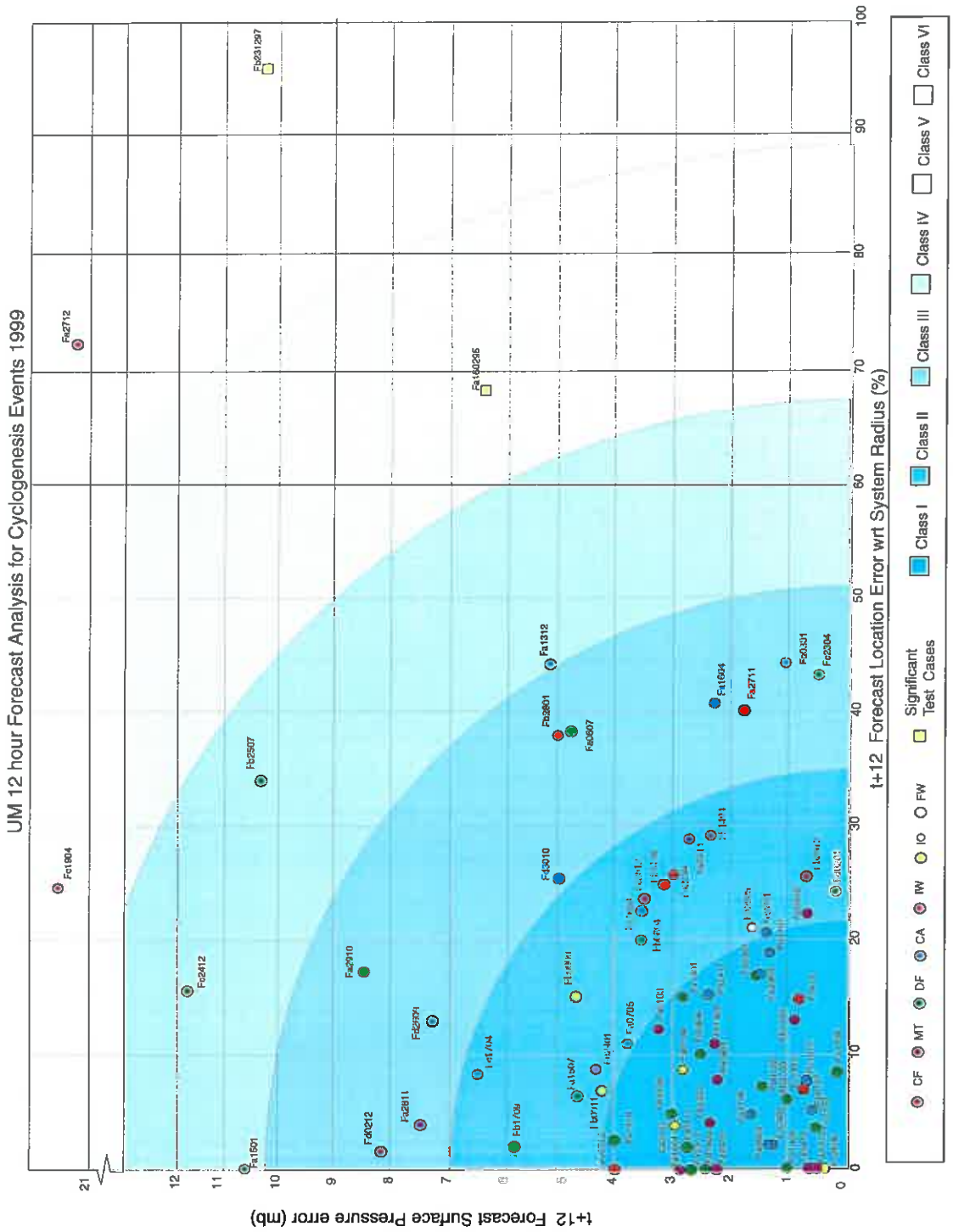

Figure 2 North Atlantic Cyclogenesis Survey 1999. The *magnitude* of the T+12 forecast surface pressure error is plotted as a function of location error (with respect to system size). The forecast results are arbitrarily divided into forecast 'classes' (I to VI) for discussion purposes. Significant test cases are also included in the figure for comparison. Each cyclone is labelled with the time (Fa, Fb, Fc, Fd refers to 00z, 06z, 12z, 18z respectively) and date (ddmm) of the start analysis. Each cyclone has been classified in terms of Young's classification scheme : Confluent flow (CF), Meridional Trough (MT), Diffluent Flow (DF), Cold Air (CA), Induced Wave (IW), Instant Occlusion (IO). The additional classification of Frontal Wave (FW) has also been included. Note the change of vertical scale at 13mb.

2.4 *Survey Results – Model Performance*

The survey consists of 74 extra-tropical cyclones that existed within the North Atlantic region during 1999. The vast majority of cyclones in the study are of a developing nature, with positive deepening analysed over the 12 hour period. A wide variety of deepening rates are observed in the cyclone characteristics, ranging from smaller to more explosive values in 12 hours.

Figure 3 shows a graph of Forecast Pressure Error v Forecast Location Error for the survey data. The data shows that most North Atlantic cyclones are forecast within 5mb of their analysed pressure and within 30% of their location 12 hours later. There is also a significant number of cyclones that are only forecast within 10mb of their analysed pressure and within 50% of their location 12 hours later. These are significant errors when one considers that the forecast range is very short.

One of the striking things that is also shown by Figure 3 is the clear bias towards positive pressure errors: 75% of the cyclones in the survey have positive pressure errors. As the pressure error has been calculated relative to the analysed pressure, this means that the model has underdeveloped 75% of forecast cyclones in the North Atlantic.

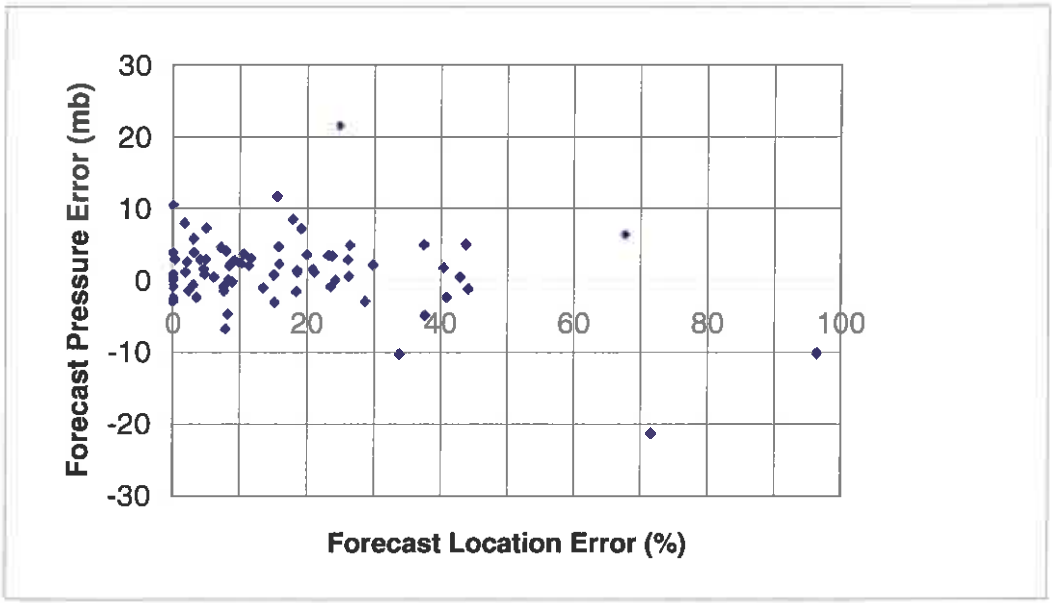

Figure 3 As Figure 2, but for *Absolute* Forecast Pressure Error (mb) v Forecast Location Error (%).

This biasing is made more apparent by the graph shown in Figure 4, which shows a plot of forecast deepening rate vs analysed deepening rate for the survey cyclones. A linear regression (with the origin as an anchor point) has been performed on the cyclone data and is included on the figure as the solid black line. The figure shows a good linear relationship between the forecast deepening rate (mb/12 hour) and the analysed deepening rate (mb/12 hour).

A perfect forecast model would result in a graph with analysed deepening rate = forecast deepening rate, and the gradient of this line would be unity (shown as a dotted line on Figure 4). However, the data shows that most cases are significantly below this line, and lie

on a line that is shallower in gradient (based on the linear regression ~0.7) than the perfect forecast, indicating a significant under-developing of cyclones by the model.

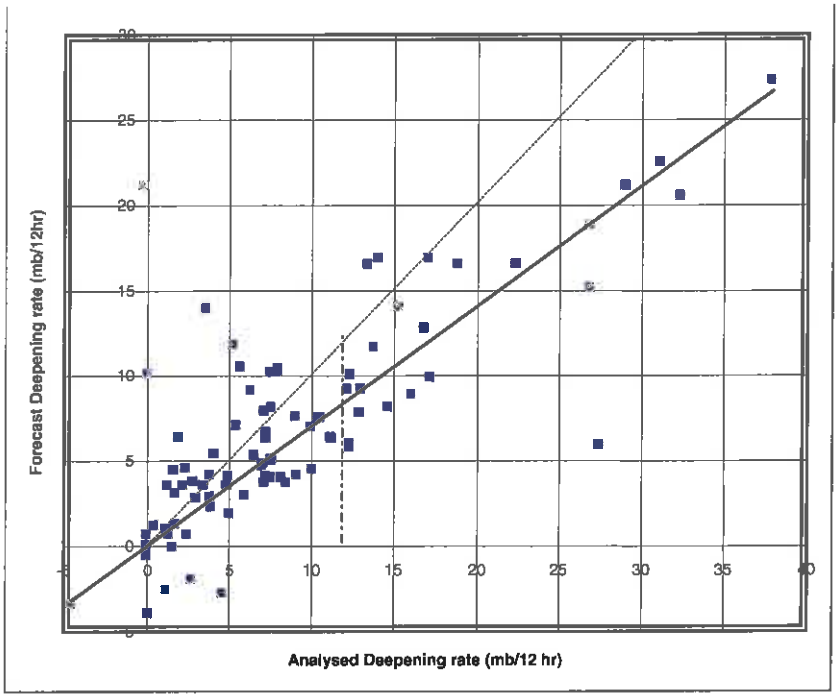

Figure 4 Forecast Deepening rate vs Analysed Deepening rate for the cyclones in the 1999 North Atlantic Survey. A linear regression fit has been performed on the data (solid line). The diagonal dotted line represents the performance of the model in an ideal forecast. The vertical dot-dash line at 12mb/12hours represents a cyclone that is defined as undergoing explosive cyclogenesis (also called a 'bomb').

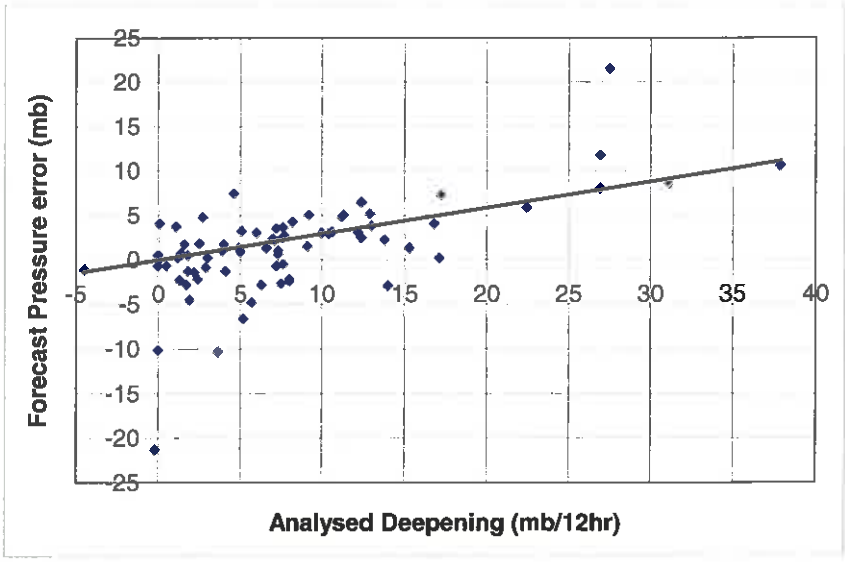

Figure 5 Forecast Pressure as a function of analysed deepening. A linear regression has been performed on the data and is shown on the figure.

The implications of this model bias in the 12 hour forecast range are large. Figure 5 shows a plot of forecast pressure error vs the analysed deepening rate, in which again, a linear regression has been performed on the data. The graph shows that the forecast pressure error increases linearly with the deepening rate of the cyclone, with the forecast pressure error ~25% the 'true' deepening rate of the cyclone in 12 hours (e.g. the expected error of a cyclone deepening at a rate of ~40mb/12 hours is approximately 10mb in that 12 hours).

Taking the definition of a 'bomb' as a deepening rate of 1mb/hour (12mb/12 hours on the graph) over a period of 24 hours, an operational forecaster should expect an under-developing of this cyclone by approximately 3mb in the first 12 hours. Assuming a linear relationship of this pressure error with forecast time (which may not necessarily be true), a 24 hour forecast of this cyclone could be underdeveloped by as much as 20mb and would therefore significantly under-predict the severity the cyclone. As the survey data indicates that 25% of extra-tropical cyclones in the North Atlantic are of this deepening rate or more, then these errors represent a significant performance error in the model.

The next section will use the survey data to assess the relationship between upper level model PV and water vapour imagery.

3 Assessment of the Potential Vorticity and Water Vapour Imagery Relationship

3.1 Choice of Potential vorticity Surface used in the Water Vapour Comparison

There are a number of ways in which PV may be displayed in order to facilitate a comparison with water vapour imagery, each method differing by the surface on which PV is displayed. The surface must be within the proximity of the tropopause in mid-latitudes as it is in mid-latitudes that the polar front exists and where the dynamics of the tropopause are involved in cyclogenesis (it is also here where the PV and WV relationship is said to hold best). Figure 6 shows the zonally averaged PV distribution in the northern hemisphere as a function of latitude. In general, tropospheric values of PV are <2.0 PV unit, whilst stratospheric values are >2.0 PV units. The tropopause may therefore be considered as being represented by the PV=2.0 surface (Hoskins et al., 1985).

Mansfield (1997) discussed several ways in which potential vorticity can be displayed and compared with water vapour imagery. Isentropic potential vorticity (IPV: PV on a potential temperature surface) is useful when one is diagnosing model performance over a period of time due to PV being conserved under these conditions. This is also a natural way of looking at PV in cyclogenesis as stratospheric air may be advected down the isentropic surfaces to altitudes well within the tropopause, and it is this process that is occurring within the dry intrusion region of a cyclone visible on water vapour imagery. For these purposes, PV on θ=315K is commonly used due to its proximity to the tropopause (PV=2) in mid-latitudes (See Figure 6). However, as Mansfield (1994,1996) explains, this conservative nature of IPV can be a disadvantage when comparing model fields with water vapour imagery of cyclones in which there are developing dry intrusions; the conserved IPV fails to highlight the descending regions of the dry intrusion because although the contrast in the satellite imagery increases within the dry intrusion, the total range of PV on the isentropic surface remains constant (as it is conserved). This method also has the disadvantage that interpretation of the PV distribution in relation to the WV image can become difficult as the relative heights of the cloud imagery and PV are varying with the decrease in height of the isentropic surface on which the PV is diagnosed. Finally, it is often difficult to chose before hand which isentropic surface is the ideal surface for that cyclone, as there is significant variety from case to case.

For static comparisons therefore, it is considered by the author that PV represented on other appropriate surfaces are best used. Mansfield (1997) compares IPV with two other methods of displaying PV: height of PV=2 surface and potential temperature on PV=2 surface (the relevance of the PV=2 surface is that it again corresponds strongly with the tropopause).

Both these methods have advantages and disadvantages depending on what information is being deduced. However, the important property of the comparison in these cases is that strong gradients in PV are identified so that these may be used to compare with the strong gradients in the water vapour image.

In this work, the author has chosen to use another alternative surface on which to display the PV: the 300mb pressure surface. The 300mb pressure surface is within the region of the tropopause in mid-latitude regions (Figure 6), and so will cut through the tropopause in the region of extra-tropical cyclones. This fulfils the requirement of identifying strong gradients of PV as the pressure level is approximately horizontal in mid-latitude regions, and so highlights the descending tropospheric air within the dry intrusion. The 300mb surface also avoids the conservative and ambiguous nature (ambiguity of the ideal isentropic surface for that cyclone) of the IPV surface method.

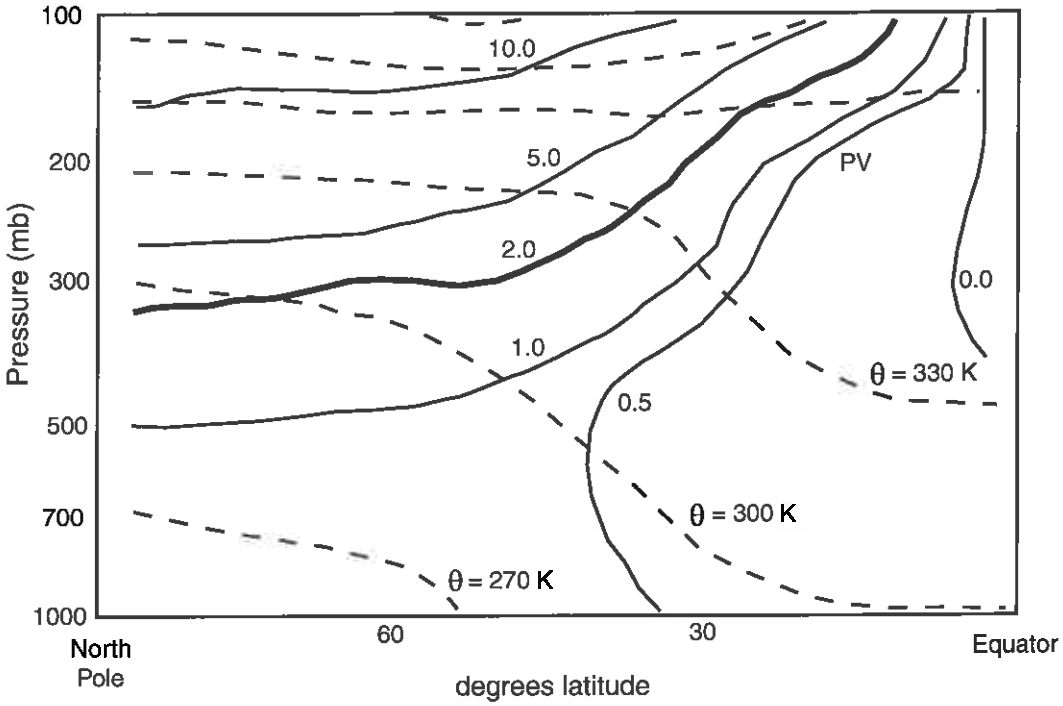

Figure 6 Average vertical PV distribution in the northern hemisphere as a function latitude (solid lines). Selected potential temperature surface are also shown (dashed lines). The tropopause corresponds to the PV=2 surface.

This method actually provides very similar results to those investigated by Mansfield (1994,1996,1997), due to the similar altitude of PV=2, the θ=315K (not shown, but midway between θ=300K and θ=330K) and the 300mb surface (see Figure 6) and often the method chosen amounts purely to personal choice.

3.2 *Features of PV and WV Comparisons*

The comparison between water vapour imagery and model potential vorticity fields is dependent on the relationship between key features in the two images. Figure 7 shows a case at 00z on the 24th October 1999 (Fa241099 in the survey). A cyclone occupies much of south western Europe, with the surface low pressure centre in north western France (not indicated). The 12 hour forecast from this analysis time was particularly good with a 0% error in location and a 2.2mb error in the forecast low mean sea level pressure.

The convention used in this work is that ascending moist air (and therefore cloud) is represented by blue/green, and descending dry air is represented by red/yellow. In relation to the figure, the frontal cloud band is therefore the blue area situated over southern France and much of central Spain. This is a particularly meridionally extended cyclone, with the cloud head almost detached from the cloud band and situated over northern France and Southern England.

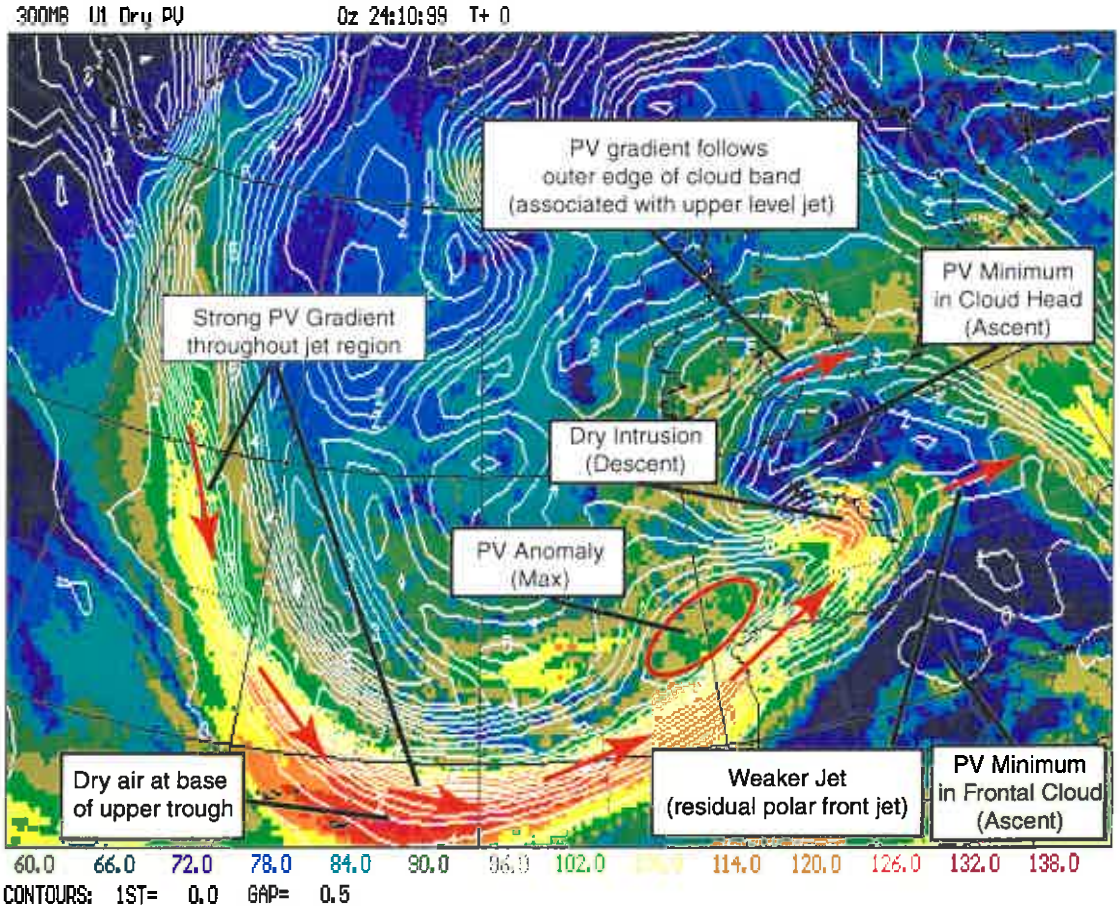

Figure 7 Key features in a water vapour image. In this work, the convention used is green/blue represents ascent and cloud, and yellow/red represents descending regions. Jet regions are denoted by the red arrows. White contours show PV on the 300mb pressure surface.

Associated with these two cloud areas of the cyclone are two PV minima. These regions are associated with diabatically produced PV in which a vertical dipole of PV is created in the troposphere; reduced values of upper level PV and increased values of lower level PV. To the rear of the system is the dry intrusion. This is identified by the much drier air descending behind the frontal cloud band from the upper troposphere/lower stratosphere and is visible

as red and yellow on the water vapour image. In the more advanced systems (such as the one shown) the dry intrusion wraps itself up between the frontal band and cloud head.

The present understanding of the relationship between PV and WV is a synthesis of many studies. These include theoretical work (e.g. Hoskins et al., 1985) and observational studies (e.g. Browning and Roberts, 1994, Browning et. al., 1996, and Mansfield 1996, 1997 - Roberts, 2000 provides a particularly authoritative discussion of PV and WV interpretation). The relationship has also been studied through conceptual model work of extra-tropical cyclones (e.g. Semple, 1998) and through personal experience as a result of the year long study documented in this work. When comparing PV fields and WV imagery, the key features examined are thus:

- The strong PV gradient associated with the polar front jet regions should correspond with the bright areas of the dry intrusion on the WV image. In the example, this is a relatively good match throughout most of the length of the dry intrusion.

- The strong PV gradient should be associated with the dry intrusion and the upper level polar front jet should lie close to, and orientated along the sharp edge of the frontal cloud band of the cyclone. In the example, this is a good match particularly to the northern half of the system (over north east Spain).

- This gradient should continue between the cloud band and cloud head, but at a substantially reduced strength. This corresponds to a weaker jet in this region that marks the residual continuous polar front jet that once flowed continuously over the cloud band in its 'leaf cloud' phase, and before any cloud head had developed. This part of the polar front jet subsides as the cloud head develops.

- The stronger part of the PV gradient should continue around the cloud head region. This effectively produces a ridge of relatively low PV (with respect to it's surroundings) that encompasses the entire cloud area of the cyclone. Within the cloud area two PV minima will develop associated with the cloud band and the cloud head.

- To the left of any polar front jet region and embedded within the dry intrusion towards the cyclone centre, a PV anomaly should exist. The PV anomaly will be associated with descent (red/yellow) to its rear and right (see Figure 7), and ascent (blue/green) to its fore and left. The anomaly should be situated to the left (in a system relative sense) of the cloud head, and close to the northern edge of the polar front jet. In this case, the ascent associated with the anomaly corresponds solely to the ascent within the cloud head. The exact relative placing of these features vary from case to case as they are often distorted by the large scale flow and evolutionary stage of the cyclone.

Section 2.3 presented the results of the cyclone survey within the context of inferring the accuracy of initial analyses. This information will be used in the following sections to subjectively observe if the 'accuracy' of the potential vorticity and water vapour comparisons discussed above vary according to the accuracy of the initial analysis.

3.3 Assessment of the PV & WV Relationship

3.3.1 Grading the PV & WV Comparisons

In order to assess the correlation between the perceived accuracy of an upper level PV/WV match, and the actual accuracy of the model analysis, the PV and WV relationship for each cyclone has been graded on a scale from 0 to 10. The basis on which this grading is made is of course highly subjective but is based upon the basic characteristics discussed in Section 3.2. (one could consider that a maximum error of +/-2 on the grading would be sufficient to allow for personal judgement). The size of the domain under which the comparison has been made has been varied so as to include the entire cyclone and a fair degree of surrounding area. Figure 8 shows three examples of PV & WV matches within Class I cyclones. The examples are labelled Good (corresponding to grades 8-10), Medium (corresponding to grades 5-7) and Poor (corresponding to grades 0-4).

The Good grades within Class I shows all features that one would hope for: the strong PV gradient corresponds closely with the dry intrusion region in the WV image, and follows the strong curvature of the cloud edge. This curvature appears to be related to the degree of deepening of the cyclone (as it is related to the degree of 'wrapping up' of the cyclone), so this is a particularly important feature to accurately represent in the model. The low values of upper tropospheric PV correctly occupy the region of the cloud band and extend gradually into the cloud head, where a PV minimum exists. The shape of the dry intrusion in relation to the surrounding cloud formation is also very well represented by the PV distribution.

The medium grades also has a good agreement between the degree of curvature of the cloud band in the image and the degree of curvature of the PV gradient. However, in this case there is a displacement of the PV contours to the east. This suggests that although the model has a reasonable representation of the severity of the cyclone (as suggested by the curvature), there is some error in the precise orientation of the particular features. Perhaps this is the origin of the fact that in going from Good to Medium in these particular cases, the pressure error remains fairly constant but the location error triples in magnitude. However, although this is true in this case the actual severity and location error will be more inter-linked than this suggests due to deepening rates themselves apparently being related to storm tracks (forecaster experience suggests more severe cyclones tend to curve north faster than less severe cyclones).

The poor grades shows a disaster in the model representation of the cyclone. The strong PV gradient is misplaced too far to the north relative to the dry intrusion region in the imagery, and also displays poor agreement in the degree of curvature of the cloud edge. This makes the model representation of the storm apparently less severe than reality. The cloud head region has correctly been represented by a PV minimum, but this is situated too far to the east in the figure. Indeed, the entire region occupied by the upper level PV anomaly shows poor agreement with the shape and distribution of the corresponding region in the water vapour image.

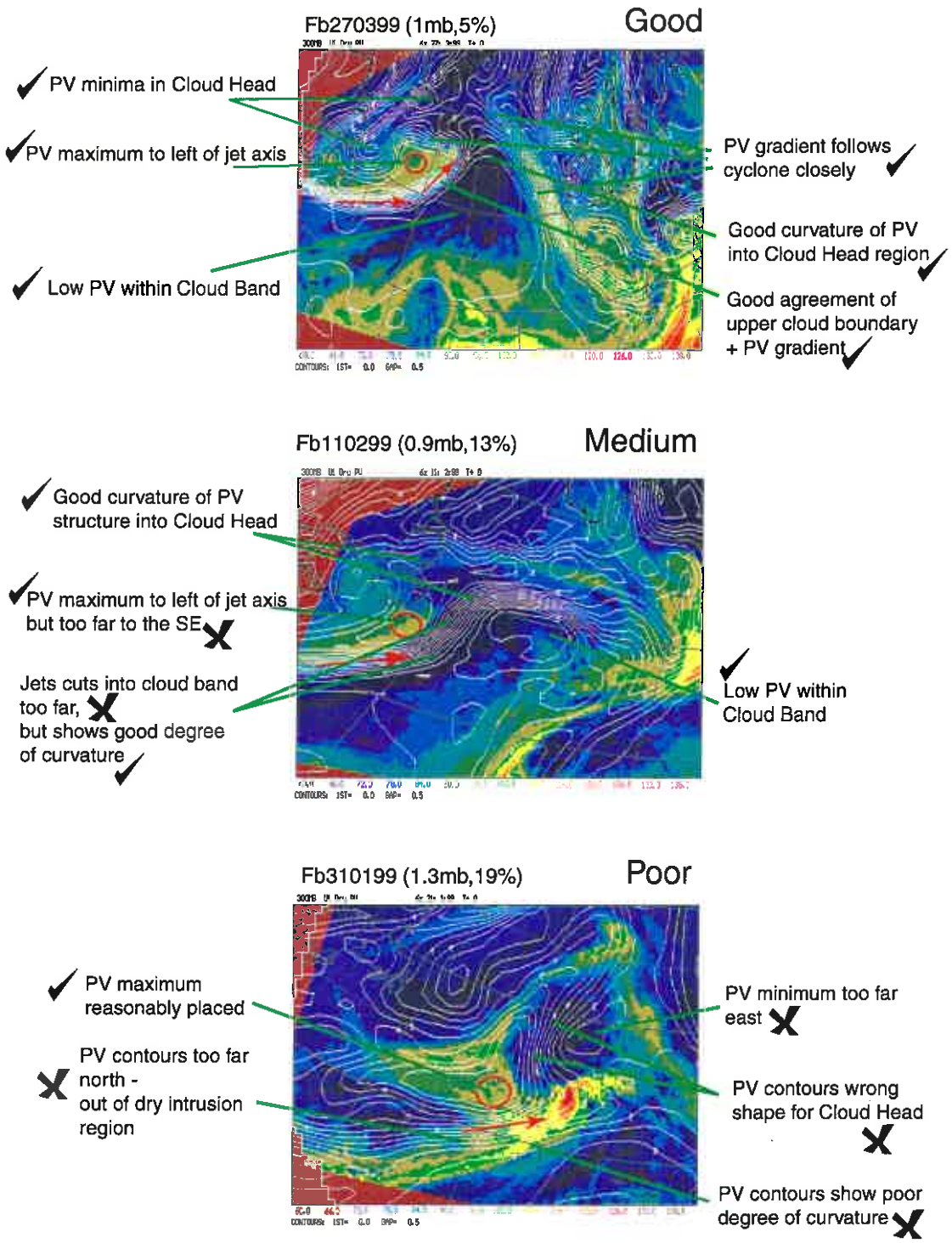

Figure 8 One example of each grade in Class I cyclones. The reasons for grading each match are shown. Grading corresponds to Good (8 to 10), Medium (5 to 7), and Poor (0 to 3).

During the course of the work it was noticed that sometimes a very good fit in one region of the image was accompanied by a poorer fit in another area of the image. The result of the subjective grading was then a fit of 'medium' (5 to 7) quality. Sections 3.3.2 and 3.3.3 therefore considers three aspects of the PV/WV fit within the grading regime. It considers the PV/WV relationship as (a) the entire region of the cyclone (the 'overall' impression), (b) the Dry Intrusion region and (c) the Cloud Head region. Categories (b) and (c) concentrate on two of the most important conceptual model aspects of the cyclonic system in terms of its development.

The 10 point grading resolution will be used in sections 3.3.2 and 3.3.3. In Section 3.3.4, the coarser Good/Medium/Poor grading resolution will be used when more general conclusions about the PV&WV are drawn with respect to the initial analysis accuracy.

3.3.2 PV & WV Grading as a Function of the Pressure Error

Figure 9 shows the overall perceived match between PV and WV as a function of the measured short period forecast pressure error. The data shows that there is a large density of data points to the lower right hand corner of the graph; 74% of cyclones have been graded with PV&WV matches >=5. Of these cases, only 3% are characterised by forecast pressure errors >5mb in 12 hours. Therefore, in 97% of cyclones in which the PV&WV match is considered as medium or good PV/WV, a good short period pressure forecast is also likely.

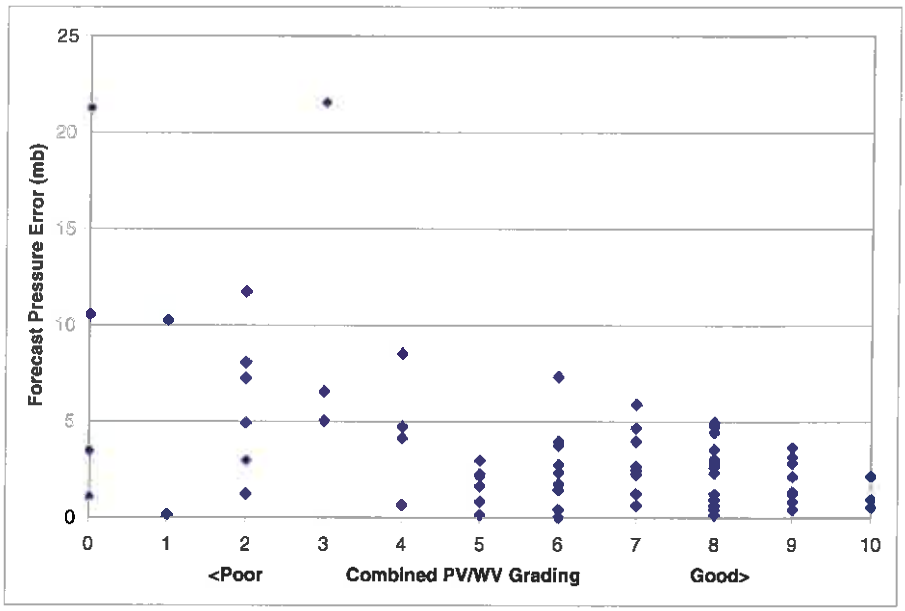

Figure 9 Overall PV & WV Grading as a function of Forecast Pressure Error.

As the PV/WV match becomes progressively worse to the left of the graph, the degree of spread increases significantly, with a shift in the density of data points to larger forecast pressure errors. Out of these poor PV&WV matches, 64% are cases in which the forecast pressure error was >=5mb in the 12 hour forecast period.

Figure 10 shows the results when only the dry intrusion is considered within the match. Once again, the graph shows a clear bias towards good grades of PV&WV matching within this region. The number of cases within grades 5 to 10 that are characterised by forecast pressure errors >5mb in the 12 hour forecast period has risen from 2 to 8. In contrast, PV&WV comparisons within the cloud head region (Figure 11) show that only 2 cases within grades 5 to 10 that are characterised by forecast pressure errors >5mb in the 12 hour forecast period. The relative density of data points in the 'poor' region of Figure 10 and Figure 11 suggest that within in the PV framework, model errors are most associated with the representation of the cloud head rather than the dry intrusion.

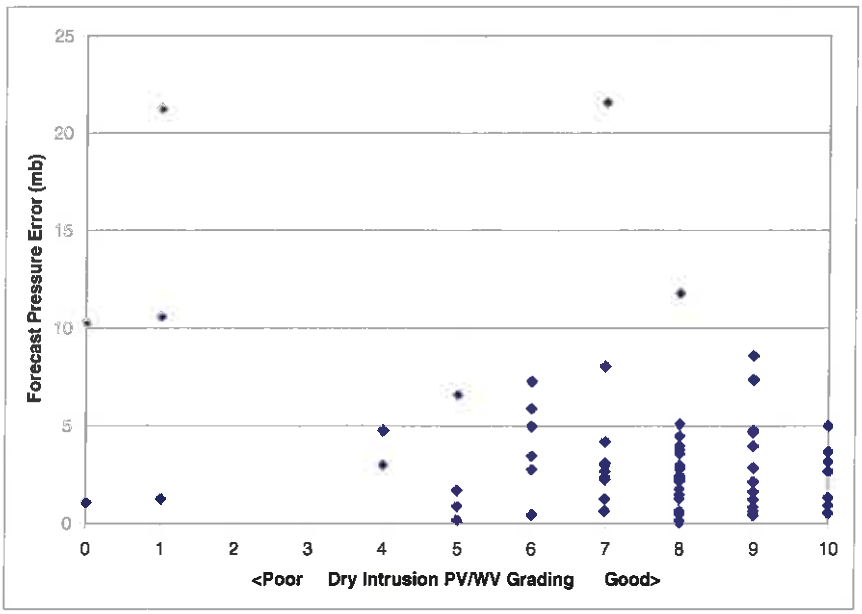

Figure 10 PV&WV grading applied only in the region of the Dry intrusion, expressed as a function of the Forecast Pressure Error.

These results do suggest that a relationship exists between the perceived accuracy of the PV and WV fit (according to the guidelines specified in Section 3.3.1) and the short period forecast pressure error. Poor matches are accompanied by a wide distribution of forecast pressure errors, with a significant and increasing probability that the forecast error will be larger as the match becomes worse.

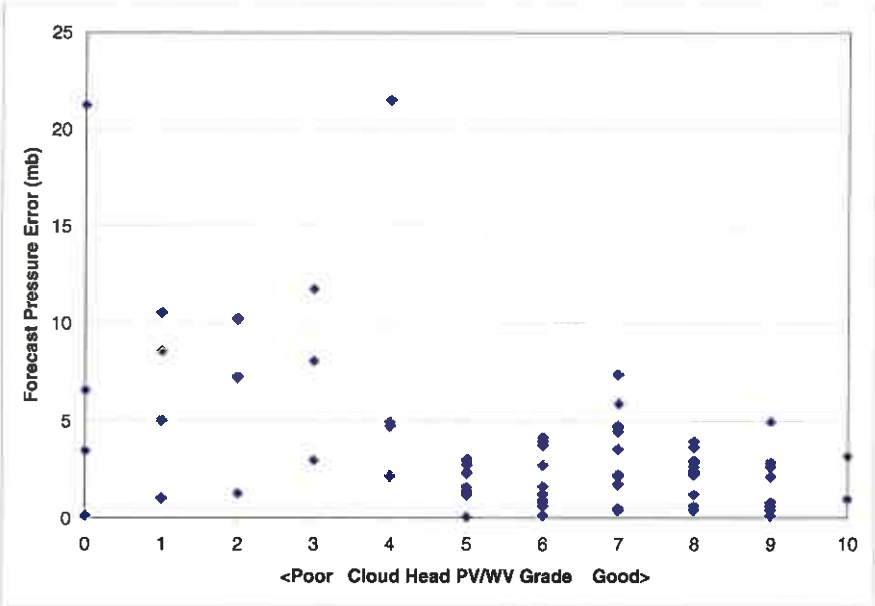

Figure 11 PV & WV grading applied only in the region of the Cloud Head, expressed as a function of Forecast Pressure Error (mb).

The next section will consider the grading of the PV&WV image and its relationship to the forecast location error of the cyclone. It will be shown that the same general characteristics are evident in the case of the location error as that of the pressure error, although the signal is more noisy.

3.3.3 PV & WV Grading as a function of the Location Error.

Figure 12 shows the results of grading the cyclone in its entirety, plotted as a function of the location error of the cyclone. The data shows that there is a large density of data points towards the bottom right hand corner of the graph. However, this graph shows that even in some apparently medium to good matches (grades 6 to 8), there are three cases which have ~40% location errors attributed to them. These cases represent about 8% of the cases with grades >=5. Thus although the spread in the location error for the medium to good cases is larger than that for the pressure error, given a medium or good PV/WV match, 92% of cyclones will be characterised by a good location error.

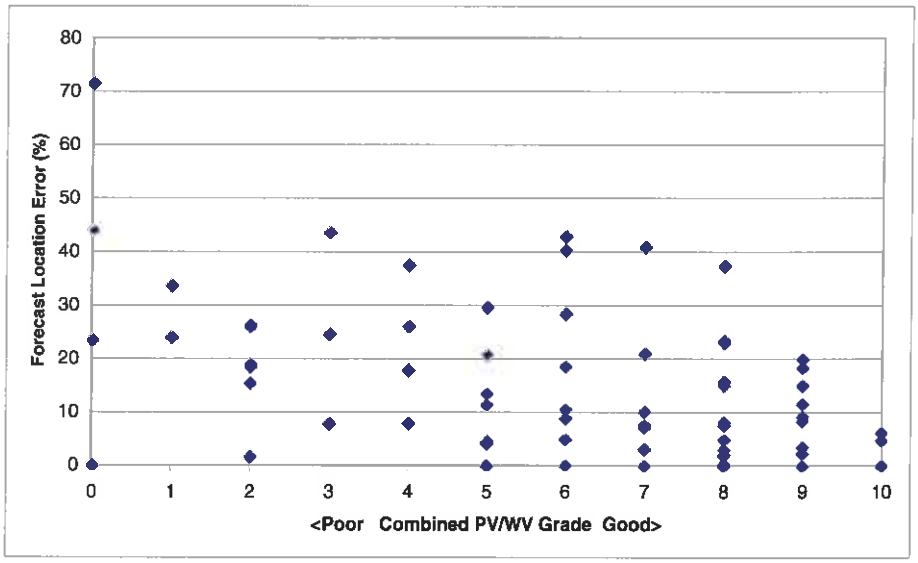

Figure 12 'Combined' PV & WV Grading as a function of Forecast Error (%).

The poorer grades show a gradual shift towards larger location errors, although there is still a relatively large spread of location errors, with approximately 40% of poor grades being characterised by relatively good forecast errors of <=20%.

When the measured location error is compared with the grading solely in the dry intrusion region of the cyclone (Figure 13), the data still displays the bias towards good grades. This indicates that in most cases, the PV/WV match shows no significant error in the representation, and this is consistent with the findings presented in section 3.3.2. Note again however, that a number of cases show poor location errors (approximately 30% of cases correspond to errors >=20%, and 8% with errors >=30%) within an apparent good grade of PV/WV match. Nevertheless, a good PV&WV match in the dry intrusion region of the cyclone corresponds with approximately 70% of location errors < 20%.

The PV/WV match within the cloud head region of the cyclone is shown in Figure 14 as a function of location error. Again, the spread is the key feature in this data, and there is probably little relationship between the two quantities based on these results.

Overall, the relationship between location error and PV&WV grading is very tenuous. The only reliable feature of the data is that the density of good PV&WV grades with small location errors is high.

In the previous section, the PV&WV grading was compared directly with the survey data in the form of pressure errors. Section 3.3.2 showed that when the forecast pressure error data was compared with the perceived PV&WV grading, the degree of spread increased

significantly as the grading became poorer. This spread meant that as the PV&WV grading became poorer, the probability of a poor forecast increased. However, it has been shown in this section that when the same analysis was carried out in regards to the forecast location error, the data trends were much more noisy.

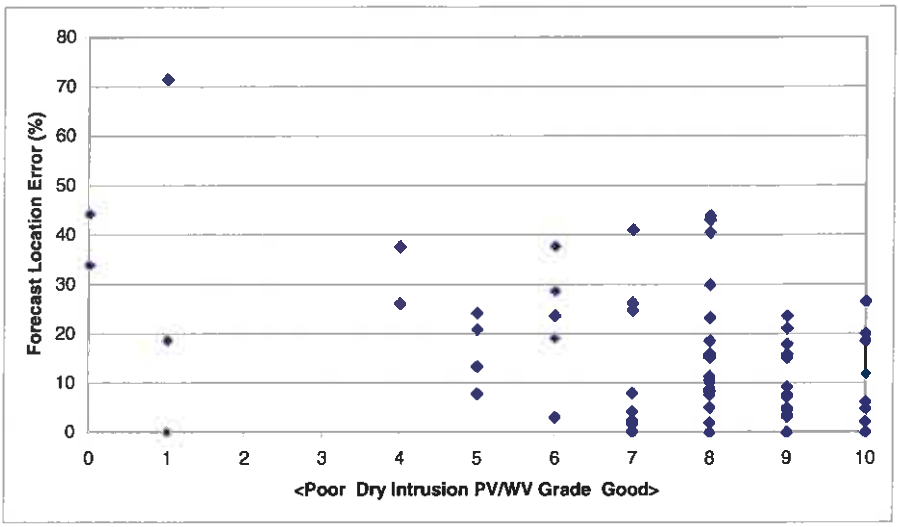

Figure 13 PV & WV Grading applied only in the region of the Dry Intrusion, expressed as a function of forecast location Error (%).

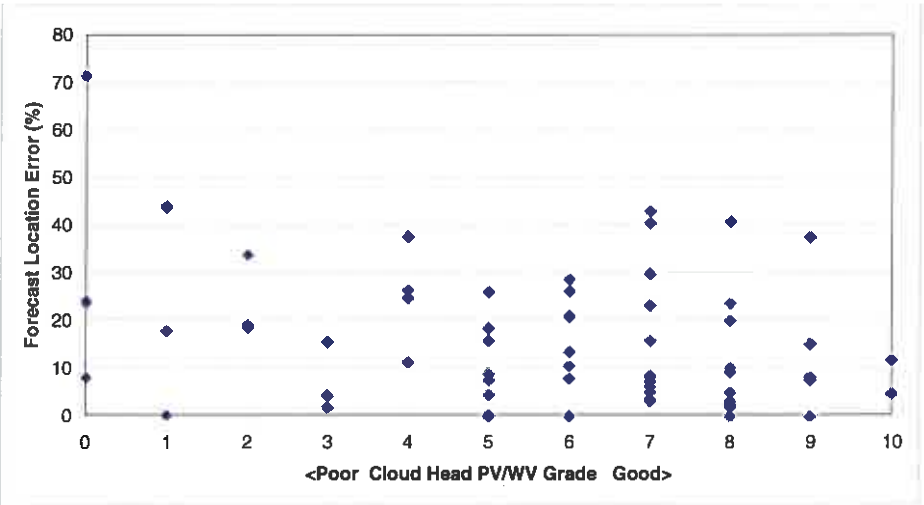

Figure 14 PV & WV Grading applied only in the region of the Cloud Head, expressed as a function of forecast location Error (%).

Perhaps the reason for this is that the location error is much more dependent on the larger scale flow than the pressure error. This is likely to make the correlation between the grading of the PV and WV within the cyclone region and the location error more noisy due to contributions from other factors outside the cyclone domain. It is more understandable that the pressure error however, should be more closely related with the individual airflows within the cyclonic system and this may be the reason why there appears to be a stronger relationship in this case.

Nevertheless, the location error statistics still show some indications of the trend as illustrated by the large density of data points at good grades and small location errors. A way of combining the pressure and location errors, and looking for more large scale changes in the grading characteristics is therefore necessary, and is considered in the next section.

3.3.4 PV & WV Comparisons within the Analysis Classes

The problem that arises when considering errors of the sort discussed in Sections 3.3.2 and 3.3.3 is that of determining a sensible way in which to combine them to get an overall indication of the forecast error. This is necessary in this case as the errors are to be used to give an indication of the probable initial analysis error, and both the pressure and location errors are meteorologically important quantities for this purpose. The pressure error is important as it relates to the severity of the cyclone and will therefore have a bearing on wind strength and precipitation etc. The location error is equally important as it relates to the track of the system and can therefore make the difference between a forecast success and a complete forecast failure for any one location.

Section 2.3 used a graphical approach to combine the errors and divided the data into broad (subjectively determined) bands. As the data was being used to infer the initial analysis accuracy, these 'classes' were designed to allow for uncertainties in the data introduced as a product of errors in the model formulation.

The difference between the pressure and location errors as discussed in sections 3.3.2 and 3.3.3 was that there was more uncertainty evident in the relationship between the PV&WV grading and the location error than between the grading and the pressure error. This was attributed to the extra uncertainty introduced by the larger scale flow on the location errors. As the gross properties of a large number of cases are studied within the cyclone classes (Section 2.3) rather than individual cases, the classes are useful in allowing for fluctuations in the data introduced as a product of the larger scale flow on the location. It was for these reasons that the graphical approach shown in Figure 2 was constructed to allow the PV&WV grading to be related to the inferred analysis accuracy. Within this framework, only 3 grades (good, medium and poor) are necessary to study the PV and WV relationship. These are related to those used previously by good (8-10), medium (5-7) and poor (0-4).

Figure 15 shows the distribution of the PV&WV grading within the analysis classes. At the top of the figure, each class is divided into its component grades (good, medium and poor). The lower half of the figure re-expresses this data in terms of the percentage of each grade relative to the total number of cyclones in that Class. For example, the top graph shows that 29 cyclones in class I are characterised by good PV and WV matches, and this equates to around 80% of the cyclones in class I as shown in the lower graph.

Thus within Class I, 80% of cyclones are considered as good PV/WV matches, whereas only 17% are considered as medium grades. Only 3% of Class I cyclones are considered as poor grades. For Class II cyclones good grades of PV/WV matches contribute 61% to the total cyclones in that class, whilst medium and poor grades contribute 22% and 17% respectively.

In Class III, the number of good PV/WV grades has reduced to 54%, whilst those of Medium and Poor grades has increased to 27% and 18%. Class IV cyclones begin to suffer from a lack of statistics. Nevertheless, out of 4 cyclones identified to be in this class, none of them are considered to be of good PV/WV match, whilst 25% and 75% are considered to be medium and poor respectively. There were no cyclones identified as Class V cyclones in the survey. Two cyclones make up Class VI, however, and of these there are one of each of medium and poor grades.

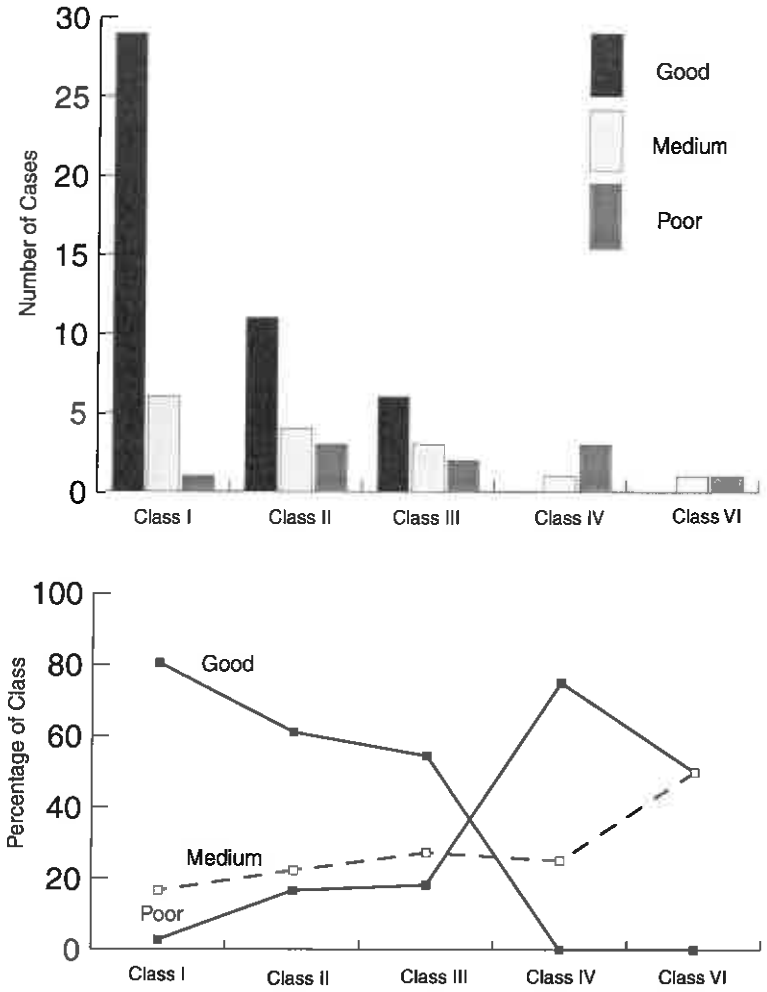

Figure 15 Grading (Good, Medium, Poor) Statistics for the PV/WV relationship as a function of T+12 forecast accuracy & inferred analysis accuracy (Class I to VI).

The large number of Class I cyclones with good PV & WV matches echo the results of sections 3.3.2 and 3.3.3 in which a large density of data points were discussed at high (good) PV and WV grades and small pressure and location errors.

This method shows the data from an interesting perspective. It shows that as the short period forecast error grows (and the cyclone class increases), then the relative proportion of good PV&WV matches reduces considerably. Also, as the class increases, the relative proportion of medium and poor grades increase. Of particular note is the absence of the good grades within class IV and VI cyclones. This is persuasive evidence therefore that there is a genuine relationship between PV and WV and the accuracy of the UM analysis.

4 Summary & Conclusions

The1999 north Atlantic Survey documented in this work was initially designed to address whether the perceived accuracy of the PV and WV relationship was reliably correlated with the actual accuracy of the UM analysis at that time. The accuracy of the initial analysis has been inferred from data that considered the short range forecasts of cyclones. By considering the T+12 forecast, it is assumed that the most probable source of error will be due to errors in the initial analysis, rather than errors in the model formulation. The forecast accuracy has been measured relative to the verifying analysis at T+12, that within the confines of the survey, is the best estimate of the true state of the atmosphere.

The results have shown that there is a correlation between PV & WV imagery and analysis/forecast accuracy. However, this correlation is not such that a poor PV&WV comparison is always correlated with a poor analysis and always leads to a poor forecast. Instead, the relationship is such that if a good PV&WV comparison is observed then it *is very likely* to be associated with a good analysis. Any reduction in the confidence of the PV&WV comparison equates to an *increased probability* that the UM analysis is in error. The results are summarised in
Table 1.

	% of cases in which PV&WV match is Perceived as Good or Medium	% of cases in which PV&WV match is Perceived as Poor
Good Pressure Forecast (<5mb error)	97%	39%
Poor Pressure Forecast (>5mb error)	3%	61%
Good Location Forecast (<20%)	82%	42%
Poor Location Forecast (>20%)	18%	58%

Table 1 Summary of results from the cyclone survey in relation to the accuracy of the PV&WV relationship.

The relationship between the accuracy of the PV&WV match and the forecast pressure error is the most clear. It has been found that a 'medium' or 'good' PV&WV match will characterise 97% of the initial analyses from which a forecast pressure error <=5mb is observed (considered for these purposes a relatively good pressure forecast), and only 3% of cases which result in a poor forecast. If the PV&WV match of the initial analysis is perceived as 'poor' it has been found that the forecast pressure error will be >5mb (considered as poor) in 61% of the cases, with 39% of cases resulting in good forecasts.

Clearly, a *good or medium PV&WV match is almost certainly an indication of a good forecast* pressure and a *poor PV&WV match will be an indication of a poor forecast* pressure ~2 out of every 3 cases.

It has also been found that the region of most importance to the development of the cyclone in these comparisons is that of the cloud head. The correlation between good comparisons in this region and good pressure forecasts is very strong.

The dependence on forecast track of the PV&WV relationship within the cyclone is less clear. If the perceived PV&WV match is considered 'medium' or 'good' then this is characterised in 82% of cases by a forecast location error <20% (considered good for these cases), and 18% of cases by a forecast location error >20%. Although not as strong as the pressure relationship discussed above, this represents a reasonably strong relationship, and one could have reasonable confidence that a *good or medium PV&WV match would be associated with a good location* forecast. If the PV&WV match is considered 'poor' there is a 58% probability that the corresponding forecast will have a poor forecast track, but still a significant 42% probability that the location error will still be <20% (and therefore considered good).

In terms of the location forecast therefore, this means that a *good PV&WV match is very likely to be associated with a good forecast location* and a *poor PV&WV match is in favour (~ 6 out of every 10 cases) of a poor location error.*

It is suggested that this reduced certainty in the correlation between PV&WV and location is due to the track of a cyclone being highly dependent on the larger scale flow around it, whilst the pressure error is more highly dependent on the local air flows in the system.

Combining the pressure and location errors, and using 'cyclone classes' to introduce a smoother distribution (considering gross properties of a large number of cyclones), the relationship between the accuracy of the PV&WV match and the inferred accuracy of the analysis is borne out. The number of good matches are observed to diminish as the analysis accuracy decreases, whilst the number of medium and poor matches are observed to increase.

The ambiguity clearly inherent in the relationship between PV&WV comparisons and the accuracy of the initial analysis (and that of the subsequent forecast) is probably in part a result of the role of lower level cyclonic development. This cannot be deduced from the water vapour imagery as the imagery only gives information about the upper part of the troposphere (subject to certain conditions discussed in Section 1) making comparisons with lower level PV impossible. However, in some cases of cyclogenesis, lower level development is likely to play an important role (to a greater or lesser degree depending on the case) so that cases in which the model had upper level PV correct and lower level PV incorrect would not be identified by the method. However, it should not be considered that upper and lower level development are completely independent of one another as each level will tend to 'feed' of each other during various stages of the cyclone evolution. For this reason, one would expect some indication of model error at some stage during cyclogenesis and highlights the importance of monitoring the PV&WV imagery over a period rather than individual instances as has been performed in this survey by necessity.

The survey data has also been used to observe the overall performance of the Unified model on cyclogenesis in the North Atlantic. The data shows that the model correctly develops cyclones with small or moderate deepening rates <12mb in 12 hours, representing about ~75% of the cyclogenesis events in the North Atlantic in 1999. However, the majority of the remaining ~25% of cases, with deepening rates >12mb (by definition, cyclones undergoing explosive cyclogenesis) in 12 hours are significantly underdeveloped by the model. It has been shown that a cyclone undergoing the minimum in explosive cyclogenesis is likely to be approximately 3mb underdeveloped after 12 hours.

However, cyclones undergoing explosive cyclogenesis can deepen at much larger rates, and this is illustrated by the data. In the more extreme cases, cyclones in 1999 have deepened by over 30mb in 12 hours. The expected error associated with cyclones of this severity is shown to be ~10mb in 12 hours. These cyclones, severely underdeveloped by the model in such a short period of time, represent a crucial area of forecasting on which the Met Office reputation is built.

5 Recommendations

This study has shown that the PV&WV relationship is correlated with the accuracy of the initial analysis and the accuracy of the forecast from that analysis. However, it has also shown that the reliability of a UM analysis should not be based solely on PV&WV comparisons, as the relationship is one of probabilities rather than rules.

However, PV&WV comparisons *are* a valuable source of information on the likely reliability of the model. On the whole, a good PV&WV match is an extremely good (>80%) indication that the model is correct in its representation of the cyclone. However, only ~60% poor matches actually correspond with poor analyses. As these apparently poor matches are those in which a forecaster would want to intervene, extreme caution should be taken when using this information to infer appropriate modifications to the model fields. It would be recommended that only in the relatively rare 'very poor' match cases, should any modification be attempted to the model field.

The ambiguity in the method probably arises in part due to the lower level development unobserved by the satellite. It is suggested that in many cases lower and upper level development will influence each other during cyclogenesis so that errors initially in the lower levels may at some stage be observed in the upper levels. For this reason it is recommended that PV&WV comparisons are made continuously and not at widely spaced intervals such as every 48 hours.

The probabilistic nature of the PV&WV relationship as observed in this study is also likely to arise due to the fact that water vapour imagery displays a depth of the troposphere the height of which is often hard to judge. This means that it is crucial that other model fields should be used when interpreting PV&WV comparisons. Of particular interest should be the distribution of PV on lower levels than 300mb so that system tilt and undercutting of the dry intrusion airstream of the cloud head (a relatively common occurrence in cyclogenesis) may be observed and that may otherwise give a false indication of an error (or not) in the comparison. Also recommended is the use of the model relative humidity field as discussed by Mansfield (1997).

The underdevelopment of explosive cyclones also discussed in this work may not necessarily be due entirely to the model formulation. As this data relates to short period forecasts, the data assimilation process may also have an influence. Further work, beyond the scope of this study would be necessary to investigate this. Nevertheless, at the present time operational forecasters should be aware of these results when interpreting model output of extra-tropical cyclones.

6 References.

Browning, K.A. & Roberts, N.M. (1994). Structure of a Frontal Cyclone. Q.J.R. Meteorol. Soc., 120: 1535-1557.

Browning, K.A. & Roberts, N.M. (1994)[2]. Use of Satellite imagery to diagnose events leading to frontal thunderstorms: part I of a case study, Meteorol. Appl. 1, 303-310

Browning, K.A., Roberts, N.M. & Sim, C.S. (1994). A mesoscale vortex diagnosed from combined satellite and model data, Meteorol. Appl. 3, 1-4.

Demirtas, M & Thorpe, A.J., (1997). Sensitivity of short-range weather forecasts to local potential vorticity modifications. JCMM Internal Report 71

Hoskins, B.J., McIntyre, M.E & Robertson, A.W. (1985). On the use and significance of isentropic potential vorticity maps. Q.J.R. Meteorol. Soc., 111: 877-946.

Mansfield, D.A (1996). The use of potential vorticity as an operational forecast tool. Meteorol. Appl. 3, 195-210

Mansfield, D.A (1997). The use of potential vorticity and water vapour imagery to validate numerical models. Meteorol. Appl. 4, 305-309

Roberts, N.M. (2000) A guide to aspects of water vapour imagery interpretation: the significance of dry regions. JCMM internal report 109 (NWP Technical Report 294).

Semple, A.T. (1998) Conceptual Model of Cyclogenesis. JCMM Internal Report 92

Semple, A.T., Saunders F.W. and Bader M.J. (2001). A study of the Christmas Eve Storm, 1997. Work to be published.

Swarbrick, S.J. (1999) Use of Water Vapour Imagery and PV Inversion to Adjust Initial Conditions in NWP, Internal Report 102

Thorpe, A. J & Volkert, H (1997). Potential Vorticity: A short history of its definitions and uses. JCMM internal report 75.

Young, M.V., Monk, G.A., Browning, K.A., Interpretation of satellite imagery of a rapidly deepening cyclone, Q.J.R. Meteorol. Soc., 113: 1089-1115.

CURRENT JCMM INTERNAL REPORTS

This series of JCMM Internal Reports, initiated in 1993, contains unpublished reports and also versions of articles submitted for publication. The complete set of Internal Reports is available from the National Meteorological Library on loan, if required.

1. **Research strategy and programme**
   K A Browning et al
   January 1993

2. **The GEWEX Cloud System Study (GCSS)**
   GEWEX Cloud System Science Team
   January 1993

3. **Evolution of a mesoscale upper tropospheric vorticity maximum and comma cloud from a cloud-free two dimensional potential vorticity anomaly**
   K A Browning
   January 1993

4. **The global energy and water cycle**
   K A Browning
   July 1993

5. **Structure of a midlatitude cyclone before occlusion**
   K A Browning and N Roberts
   July 1993

6. **Developments in systems and tools for weather forecasting**
   K A Browning and G Szejwach
   July 1993

7. **Diagnostic study of a narrow cold frontal rainband and severe winds associated with a stratospheric intrusion**
   K A Browning and R Reynolds
   August 1993

8. **Survey of perceived priority issues in the parametrizations of cloud-related processes in GCMs**
   K A Browning
   September 1993

9. **The effect of rain on longwave radiation**
   I Dharssi
   September 1993

10. **Cloud microphysical processes - a description of the parametrization used in the large eddy model**
    H Swann
    October 1993

11. **An appreciation of the meteorological research of Ernst Kleinschmidt**
    A J Thorpe
    May 1992

12. **Potential vorticity of flow along the Alps**
    A J Thorpe, H Volkert and Dietrich Heimann
    August 1992

13. **The representation of fronts**
    A J Thorpe
    January 1993

14. **A parametrization scheme for symmetric instability: test for an idealised flow**
C S Chan and A J Thorpe
February 1993

15. **The Fronts 92 Experiment: a Quicklook Atlas**
Edited by T D Hewson
November 1993

16. **Frontal wave stability during moist deformation frontogenesis**
Part 1: Linear wave dynamics
C H Bishop and A J Thorpe
May 1993

17. **Frontal wave stability during moist deformation frontogenesis**
Part 2. The suppression of non-linear wave development
C H Bishop and A J Thorpe
May 1993

18. **Gravity waves in sheared ducts**
S Monserrat and A J Thorpe
October 1993

19. **Potential vorticity and the electrostatics analogy: quasi-geostrophic theory**
C Bishop and A J Thorpe
November 1993

20. **Recent advances in the measurement of precipitation by radar**
A J Illingworth
April 1993

21. **Micro-physique et givrage: cloud microphysics and aircraft icing**
A J Illingworth
May 1993

22. **Differential phase measurements of precipitation**
M Blackman and A J Illingworth
May 1993

23. **Estimation of effective radius of cloud particles from the radar reflectivity**
N I Fox and A J Illingworth
May 1993

24. **A simple method of Dopplerising a pulsed magnetron radar**
A Hua, A J Illingworth and J Eastment
November 1993

25. **Radiation and polar lows**
George C Craig
February 1994

26. **Collected preprints submitted to the International Symposium on the Life Cycles of Extratropical Cyclones; Bergen, Norway, 27 June - 1 July 1994**
April 1994

27. **Convective frontogenesis**
Douglas J Parker and Alan J Thorpe
April 1994

28. **Improved measurement of the ice water content in cirrus using a total water evaporator**
Philip R A Brown and Peter N Francis
April 1994

29. **Mesoscale effects of a dry intrusion within a vigorous cyclone**
K A Browning and B W Golding
April 1994

30. **GEWEX Cloud System Study, Science Plan**
May 1994

31. **Parametrization of momentum transport by convectively generated gravity waves**
R Kershaw
May 1994

32. **Mesoscale Modelling Newsletter No 5**
May 1994

33. **Observations of the mesoscale sub-structure in the cold air of a developing frontal cyclone**
K A Browning, S A Clough, C S A Davitt, N M Roberts and T D Hewson
May 1994

34. **Longwave radiative forcing of a simulated tropical squall line**
Imtiaz Dharssi
July 1994

35. **On the nature of the convective circulation at a kata-cold front**
K A Browning
September 1994

36. **Collective preprints of papers submitted to the COST-75 International Seminar on Advanced Weather Radar Systems, Brussels, 20-23 September 1994**
November 1994

37. **Use of satellite imagery to diagnose events leading to frontal thunderstorms: Parts I and II of a case study**
K A Browning and N M Roberts
November 1994

38. **The role of spaceborne millimetre-wave radar in the global monitoring of ice cloud**
P R A Brown, A J Illingworth, A J Heymsfield, G M McFarquhar, K A Browning and M Gosset
December 1994

39. **Potential vorticity inversion**
Michal Ziemianski
October 1994

40. **Theory of mature tropical cyclones; a comparison between Kleinschmidt (1951) and Emanuel (1986)**
Suzanne L Gray
December 1994

41. **Dispersion and removal of pollutants during the passage of an atmospheric frontal system**
N R Gimson
December 1994

42. **The role of snow sublimation in frontogenesis**
D J Parker and A J Thorpe
December 1994

43. **Potential vorticity and the electrostatics Analogy: Ertel-Rossby formulation**
A J Thorpe and C H Bishop
December 1994

44. **Mesoscale aspect of extratropical cyclones: an observational perspective**
K A Browning
January 1995

45. **A polar low outbreak: evolution and mesoscale structures**
T D Hewson, G C Craig and C Claud
February 1995

46. **Generation of near-surface gusts of deep convection**
K Nakamura and R Kershaw
April 1995

47. **Attribution concepts applied to the Omega Equation**
S A Clough, C S A Davitt and A J Thorpe
June 1995

48. **Parametrization of mixed-phase cloud and precipitation**
Susan P Ballard and M Gerard Hutchinson
June 1995

49. **Short-range forecasting of stratocumulus: initialization prediction**
Susan P Ballard, Simon D Jackson and B Macpherson
June 1995

50. **Contributions of the JCMM/Dept of Meteorology Radar Group to the 27th AMS Radar Meteorology Conference, Vail October 1995**
June 1995

51. **Cold pools in shear**
Douglas J Parker
September 1995

52. **High-resolution analysis of frontal fracture**
K A Browning, S P Ballard and C S A Davitt
September 1995

53. **The albedo of broken cloud fields: calculations using a modified two stream radiation code**
Imtiaz Dharssi and Roy Kershaw
October 1995

54. **Parametrization of momentum transport by convection. I: theory and cloud modelling results**
R Kershaw and D Gregory
November 1995

55. **Variation of frontal structure along a cold front**
K A Browning and N M Roberts
November 1995

56. **Secondary frontal waves**
Douglas Parker
December 1995

57. **Objective fronts**
T D Hewson
March 1996

58. **Mesoscale analysis of the activation of a cold front during cyclogenesis**
K A Browning, N M Roberts and A J Illingworth
June 1996

59. **Investigation of different representations of rain in a 1-d evaporation model**
H Swann
May 1996

60. **Parametrization of diabatic processes in the inversion of the omega-equation**
M Athanassiadou and A J Thorpe
June 1996

61. **The role of the environmental flow in the development of secondary frontal cyclones**
I A Renfrew, A J Thorpe and A Joly
June 1996

62. **Consequences of the geostrophic momentum approximation on barotropic instability**
S Malardel, A J Thorpe and A Joly
June 1996

63. **Contributions to the AMS/RMS Conference on Mesoscale Processes**
Reading, 9-13 September 1996

64. **Vorticity and potential vorticity in stratified flows interacting with an isolated obstacle**
Jorge A Gutiérrez and A J Thorpe
September 1996

65. **Triple point development: two case studies**
Douglas Parker
September 1996

66. **Radar observations of wind-shear splitting within evolving atmospheric Kelvin-Helmholtz billows**
D Chapman and K A Browning
April 1997

67. **Cold frontal structure derived from radar wind profilers**
K A Browning, D Jerrett, J Nash, T Oakley and N M Roberts
May 1997

68. **The dry intrusion and its effect on the frontal, cloud and precipitation structure of extratropical cyclones**
K A Browning - Text of invited special lecture at the Spring Conference
of the Meteorological Society of Japan, University of Tsukuba, 22 May 1997

69. **Met. Office Unified Model data, diagnostics, graphics programs, and other observational data available from the JCMM through the aegis of the Universities Weather Research Network (UWERN).** (Plus supplement)
Peter Panagi and Ed Dicks
June 1997

70. **Contributions of the JCMM/Dept of Meteorology Radar Group to the 28th AMS Radar Meteorology Conference.** Austin, Texas
September 1997

71. **Sensitivity of short-range weather forecasts to local potential vorticity modifications**
Meral Demirtas and Alan Thorpe
July 1997

72. **Objective identification of frontal wave cyclones**
T D Hewson
August 1997

73. **Attribution and its application to mesoscale structure associated with tropopause folds**
A J Thorpe
September 1997

74. **The role of the environmental flow in the development of secondary frontal cyclones**
Ian A Renfrew, Alan J Thorpe and Craig H Bishop
September 1997

75. **Potential vorticity: a short history of its definitions and uses**
Alan J Thorpe and Hans Volkert
September 1997

76. **Superposing semi-geostrophic potential vorticity anomalies**
H R Birkett and A J Thorpe
September 1997

77. **Short period forecasting of catchment-scale precipitation.**
Part 1: the role of Numerical Weather Prediction
M A Pedder, M Haile and A J Thorpe
September 1997

78. **Verification of the tracking technique used in an experimental cloud motion wind inferring system**
Z Wang, K A Browning and G A Kelly
October 1997

79. **A preliminary study of Fourier series analysis for cloud tracking with GOES high temporal resolution images**
Z Wang
October 1997

80. **Analysis of an ex-tropical cyclone after reintensifying as a warm-core extratropical cyclone**
K A Browning, G Vaughan and P Panagi
November 1997

81. **A JCMM overview of FASTEX IOPs**
S A Clough, H W Lean, N M Roberts, H Birkett, J-P Chaboureau, R Dixon, M Griffiths, T D Hewson and A Montani
January 1998

82. **Programs for PV inversion and modification**
Meral Demirtas
December 1997

83. **Release of potential shearing instability in warm frontal zones**
D Chapman and K A Browning
February 1998

84. **The European Cloud-Resolving Modelling Programme (EUCREM)**
Summary Report from the coordinator
P W White
April 1998

85. **A frontal wave database**
T D Hewson
April 1998

86. **Layering observed in dropsoundings from IOP 1 of Fronts 92**
S A Clough
May 1998

87. **Use of wind-shear displays for Doppler radar data**
D Chapman and K A Browning
May 1998

88. **Radar estimates of rainfall rates at the ground in bright band and non-bright band events**
T J Smyth and A J Illingworth
June 1998

89. **Correction for attenuation of radar reflectivity using polarisation data**
T J Smyth and A J Illingworth
June 1998

90. **The effects of convection on chemical reactions and precipitation scavenging**
Neil R Gimson
July 1998

91. **How to use the display program DISP**
Nigel Roberts
August 1998

92. **Conceptual models of cyclogenesis**
Adrian T Semple
August 1998

93. **Observations of oblate hail using dual polarisation radar and implications for hail detection schemes**
T J Smyth, T M Blackman and A J Illingworth
September 1998

94. **The semigeostrophic diagnosis of vertical motion. Part I: Formulation and co-ordinate transformations**
Mike A Pedder and Alan J Thorpe
September 1998

95. **The semigeostrophic diagnosis of vertical motion. Part II: Results for an idealised baroclinic wave life cycle**
Alan J Thorpe and Mike A Pedder
September 1998

96. **Convective destabilisation by a tropopause fold diagnosed using potential vorticity inversion**
Morwenna Griffiths, Alan Thorpe and Keith Browning
October 1998

97. **Forecast skill of the ECMWF model using targeted observations during FASTEX**
A Montani, A J Thorpe, R Buizza and P Unden
October 1998

98. **Observations and model simulations of the FASTEX IOP 16 frontal wave - effects of sublimation**
Sid A Clough, Humphrey W Lean, Nigel M Roberts and Richard M Forbes
December 1998

99. **The application of conceptual models in NWP**
Adrian T Semple
January 1999

100. **Mesoscale analysis of arc rainbands in a dry slot**
K A Browning and N M Roberts
January 1999

101. **Interaction of mesoscale tropopause depressions with a warm-core cyclone: observational and model analyses, and sensitivity to analysis errors**
K A Browning, A J Thorpe, A Montani, D Parsons, M Griffiths, P Panagi and E M Dicks
February 1999

102. **The use of water vapour imagery and PV inversion to adjust initial conditions in NWP**
Sean J Swarbrick
February 1999
This report is no longer available; see Internal Report No.108

103. **Summary notes for a lecture course on Waves in the Atmosphere and Ocean**
A A White
March 1999

104. **Results of a questionnaire on the operational value of conceptual models (CMs) of fronts and cyclones**
N M Roberts & M V Young
July 1999

105. **Contributions to the Poster Session at the 1998 UWERN Annual Science Meeting**
assembled by A A White
August 1999

106. **The objective analysis of dropsonde data from FASTEX**
Richard Forbes, Sid Clough, Mark Dixon, Andy Macallan & Nigel Roberts
January 2000

107. *NWP Technical Report No.302*
Implications for Mesoscale Modelling from a Study of the FASTEX IOP 16 Mid-latitude Cyclone
Richard M Forbes, Humphrey W Lean, Nigel M Roberts and Peter A Clark
March 2000

108. *NWP Technical Report No.291*
The use of water vapour imagery and PV inversion to adjust initial conditions in NWP
Final Project Report
Sean J Swarbrick
September 1999

109. *NWP Technical Report No.294*
A guide to aspects of water vapour imagery interpretation: the significance of dry regions
Nigel M Roberts
January 2000

110. *NWP Technical Report No.300*
The relationship between water vapour imagery and thunderstorms
Nigel M Roberts
February 2000

111. *NWP Technical Report No.293*
Holomorphic structures in hydrodynamical models of nearly geostrophic flow
V N Roubtsov and I Roulstone
January 2000

112. *NWP Technical Report No.301*
Multi-sensor synthesis of the mesoscale structure of a cold-air comma cloud system
K A Browning, P Panagi and E M Dicks
March 2000

113. *NWP Technical Report No.307*
Observations of stratospheric air entering the circulation of a polar low
K A Browning and E M Dicks
May 2000

114. *NWP Technical Report No.309*
Wind profiler – Unified Model comparison statistics
Peter Panagi & Ed Dicks
March 2000

115. *NWP Technical Report No.310*
Towards a similarity theory of moist convective updrafts
Olaf Stiller and George C Craig
May 2000

116. *NWP Technical Report No.312*
The mystery of striated cloud heads in satellite imagery
R S Dixon, K A Browning and G J Shutts
April 2000

117. *NWP Technical Report No.313*
MDIAG: a Fortran 90 program to compute diagnostics on pressure levels from Unified Model data on model levels
Peter Panagi
June 2000

118. *NWP Scientific Paper No.56*
Rearrangements of functions with applications to meteorology and ideal fluid flow
R J Douglas
June 2000

119. *NWP Technical Report No.320*
Tests of New Dynamics Model on the FASTEX IOP16 case
Humphrey Lean
September 2000

120. *NWP Scientific Paper 57*
A classification of FASTEX cyclones using a height-attributable QG vertical motion diagnostic
A C L Deveson, K A Browning, T D Hewson
September 2000

121. *NWP Scientific Paper 59*
Measurements of dissipation rate in frontal zones
D.Chapman, K A Browning
August 2000

122. *NWP Technical Report 331*
Not Issued yet

123. *NWP Technical Report 337*
A Case Study of High Resolution Fog Forecasts with the New Dynamics
P. Clark
November 2000

124. *NWP Technical Report 338*
Comparison of ECMWF Winter-Season Cloud Fraction with Radar Derived Values
Robin J. Hogan, Christian Jakob, Anthony J. Illingworth
January 2001

125. *NWP Technical Report 339*
Deriving Cloud overlap statistics from radar
Robin J. Hogan, Anthony J. Illingworth
January 2001

126. *NWP Technical Report 344*
Results from simulations of an organised convective event using the New Dynamics at 12, 4 and 2km resolution.
Nigel Roberts
January 2001

127 *NWP Technical Report 348*
A North Atlantic Survey of Cyclogenesis in 1999: Unified Model Performance in Short Range Forecasts & The Relationship Between Potential Vorticity, Water Vapour Imagery and Analysis Accuracy.
Adrian Semple
March 2001

Met Office Joint Centre for Mesoscale Meteorology Department of Meteorology
University of Reading PO Box 243 Reading RG6 6BB United Kingdom
Tel: +44 (0)118 931 8425 Fax: +44 (0)118 931 8791
www.metoffice.com